Interaction of Relativistic Electron-Vortex Beams with Few-Cycle Laser Pulses

Armen G. Hayrapetyan,[1,2,*] Oliver Matula,[1,3] Andrea Aiello,[2,4] Andrey Surzhykov,[5] and Stephan Fritzsche[5,6]
[1] *Physikalisches Institut, Ruprecht-Karls-Universität Heidelberg, 69120 Heidelberg, Germany*
[2] *Max-Planck-Institut für die Physik des Lichts, 91058 Erlangen, Germany*
[3] *GSI Helmholtzzentrum für Schwerionenforschung, 64291 Darmstadt, Germany*
[4] *Institute for Optics, Information and Photonics, Universität Erlangen-Nürnberg, 91058 Erlangen, Germany*
[5] *Helmholtz-Institut Jena, 07743 Jena, Germany*
[6] *Theoretisch-Physikalisches Institut, Friedrich-Schiller-Universität Jena, 07743 Jena, Germany*
(Received 25 November 2013; published 2 April 2014; publisher error corrected 2 April 2014)

We study the interaction of relativistic electron-vortex beams (EVBs) with laser light. Exact analytical solutions for this problem are obtained by employing the Dirac-Volkov wave functions to describe the (monoenergetic) distribution of the electrons in vortex beams with well-defined orbital angular momentum. Our new solutions explicitly show that the orbital angular momentum components of the laser field *couple* to the total angular momentum of the electrons. When the field is switched off, it is shown that the laser-driven EVB coincides with the field-free EVB as reported by Bliokh *et al.* [Phys. Rev. Lett. **107**, 174802 (2011)]. Moreover, we calculate the probability density for finding an electron in the beam profile and demonstrate that the center of the beam is *shifted* with respect to the center of the field-free EVB.

DOI: 10.1103/PhysRevLett.112.134801 PACS numbers: 41.85.-p, 03.65.Pm, 42.50.Tx

Introduction.—In the beginning of the 1920s, Uhlenbeck and Goudsmit introduced the concept that electrons possess a spin angular momentum (SAM) of magnitude $\hbar/2$, in units of Planck's famous constant $h = 2\pi\hbar$, a fundamental degree of freedom for quantum particles with no classical analogue [1]. Since then the properties of the electron spin and its influence upon different elementary and complex processes have been studied extensively, both in theory [2] and in experiments [3].

Apart from the spin degree of freedom, Bliokh and co-workers [4] have shown that electron beams may carry also a nonzero orbital angular momentum (OAM) along their axis of propagation. During recent years, such electron-vortex beams (EVBs) [5,6] with an OAM projection of up to $200\hbar$ and energy $\sim$200–300 keV [7] have been produced and applied, for instance, to enhance the resolution in studying magnetic and biological materials [8] and to further explore the scattering of electrons [9]. Moreover, Bliokh *et al.* have demonstrated that both the SAM and the OAM of the electron give rise to an intrinsic spin-orbit interaction (SOI) in free EVBs [4]. The concept of intrinsic SOI stems from light beams [10,11], commonly known as either "twisted photons" or "optical vortices" that are widely investigated in the literature [12–14].

In this Letter, we study how the intrinsic SOI of the EVB is modified within a linearly polarized, few-cycle laser pulse. To achieve this, we generalized the field-free solutions of the EVB as reported in Ref. [4] for (electron) vortex beams in the field of a linearly polarized laser. Based on these generalized solutions, we demonstrate the *shift* of the center of the field-affected EVB with respect to the center of the field-free EVB. We also show that a nonzero probability can remain for finding an electron at the center of the initially (field-)free beam due to the electron-laser coupling. Below, we use relativistic Gaussian units $c = 1$, $\hbar = 1$ and write the scalar product of any two four-vectors $a = (a^0, \boldsymbol{a})$ and $b = (b^0, \boldsymbol{b})$ as $(ab) \equiv a^\mu b_\mu \equiv a^0 b^0 - \boldsymbol{a}\cdot\boldsymbol{b}$, where $\mu \in \{0, 1, 2, 3\}$.

EVB from the Dirac-Volkov solution.—We consider an electron with mass m that moves in the field of a plane-wave laser with a wave four-vector $k^\mu = (\omega, \boldsymbol{k})$ and the dispersion relation $k^2 = 0$. For such an electromagnetic field, the four-potential only depends on the scalar product of k^μ and the four-coordinate $x^\mu = (t, \boldsymbol{r})$, namely $A^\mu = A^\mu(\zeta)$ with $\zeta \equiv (kx) = \omega t - \boldsymbol{k}\cdot\boldsymbol{r}$ being the laser *phase*, and satisfies the Lorenz gauge condition $(kA) = 0$ [15]. The Dirac equation of an electron that is coupled to an external electromagnetic field is given by [15]

$$[(\hat{p} - eA)^2 - m^2 - ieF_{\mu\nu}\sigma^{\mu\nu}/2]\psi = 0, \quad (1)$$

where $\hat{p}^\mu = (i\partial_t, -i\nabla)$ is the electron four-momentum operator, $e = -|e|$ is the electron charge, $F_{\mu\nu} = \partial_\mu A_\nu - \partial_\nu A_\mu$ is the electromagnetic field tensor, $2\sigma^{\mu\nu} = \gamma^\mu\gamma^\nu - \gamma^\nu\gamma^\mu$, where γ^μ are the 4×4 Dirac matrices. For a plane-wave field A, the exact solution of Eq. (1) is known to have the (so-called) Dirac-Volkov form [15]

$$\psi_p(x) = \left[1 + \frac{e}{2(kp)}(\gamma k)(\gamma A)\right]\frac{u_p}{\sqrt{2\mathcal{E}}}e^{iS}. \quad (2)$$

Here the electron four-momentum and the mass are related via the (standard) energy-momentum relation $p^2 = \mathcal{E}^2 - \boldsymbol{p}^2 = m^2$ where $\mathcal{E}$ and $\boldsymbol{p}$ are the energy and the momentum of the electron, respectively. The exponent $S = -(px) - \mathcal{F} + \mathcal{G}$, with

$$\mathcal{F} \equiv \int_0^\zeta d\zeta' \frac{e(pA(\zeta'))}{(kp)}, \qquad \mathcal{G} \equiv \int_0^\zeta d\zeta' \frac{e^2A^2(\zeta')}{2(kp)}, \tag{3}$$

is proportional to the classical action of an electron within a plane-wave electromagnetic field [16]. Moreover, the bispinors u_p are the positive energy-momentum eigenstates of the free Dirac equation that describe both the spin-up and spin-down polarized states. These spin states of an electron are chosen to be the eigenstates $w^s = (\alpha, \beta)^T$ of the σ_z operator with eigenvalues $s = \pm 1/2$ as also considered in Ref. [4] and in contrast to Ref. [17] where the basis states of polarization are chosen to be the helicity eigenstates of $\boldsymbol{\sigma} \cdot \boldsymbol{p}/(2p)$. Our particular choice of the basis states for the spin is natural for massive particles [4,10].

An EVB is defined as a (twisted) state with a well-defined energy $\mathcal{E}_0$, longitudinal momentum $p_{\parallel 0}$, absolute value of the transverse momentum $p_{\perp 0}$, and the (quantized) projection ℓ of the OAM on the electron propagation axis [see, e.g., Refs. [4,17]]. EVBs exhibit a particular phase structure that is incorporated by the (vortex) phase factor $e^{i\ell\phi}$ in the "spectrum" of the Bessel beam

$$\tilde{\psi}_\ell(\boldsymbol{p}) = \delta(p_\perp - p_{\perp 0}) \frac{e^{i\ell\phi}}{2\pi i^\ell p_{\perp 0}}, \tag{4}$$

where $\phi \in [0, 2\pi)$ is the azimuthal angle. Equation (4) means that the electron has a *monoenergetic* distribution of the momentum over some cone with slant length $p_0 =$ const. and fixed polar (opening) angle θ_0 with regard to the propagation axis of the beam [cf. Fig. 1, blue sketch]. The opening angle of this cone is defined as $p_{\parallel 0} = p_0 \cos\theta_0$ and $p_{\perp 0} = p_0 \sin\theta_0$. Using cylindrical coordinates in momentum space, $\boldsymbol{p} = (p_\perp, \phi, p_\parallel) = (p\sin\theta, \phi, p\cos\theta)$, we construct the *Volkov-Bessel* states from the Dirac-Volkov solutions, Eq. (2), as

$$\Psi_\ell(x) = \int \tilde{\psi}_\ell(\boldsymbol{p}) \psi_p(x) p_\perp dp_\perp d\phi, \tag{5}$$

with the distribution of momentum given by Eq. (4).

To evaluate the integral Eq. (5), we apply here cylindrical coordinates $\boldsymbol{r} = (r, \varphi, z)$ in real space and restrict ourselves to a "head-on" scenario, in which the electrons and the linearly polarized photons propagate antiparallel to each other [cf. Fig. 1]. For this geometry, we choose the z axis

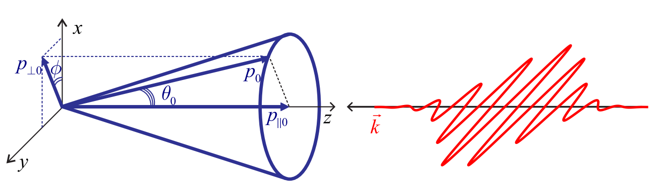

FIG. 1 (color online). Geometry of head-on collision of a relativistic EVB (with a momentum distribution indicated in blue) and linearly polarized, few-cycle laser pulse (red waveform).

directed along the propagation of the electrons which implies that the laser propagates backward along z: $\zeta = \omega t + kz$. We also choose y to be the polarization axis of photons, i.e., $A^\mu = (0, 0, A(\zeta), 0)$, where—for the moment—we do not specify the shape of $A(\zeta)$. For this linearly polarized field, the exponent $\mathcal{F}$ [cf. Eq. (3)] contributes into the dynamics of the EVB via the $p_\perp$- and ϕ-dependent term $p_\perp A \sin\phi$. Whereas, the exponent $\mathcal{G}$ is independent of both $p_\perp$ and ϕ, since its denominator $(kp) = \omega\mathcal{E} + kp_\parallel$. Furthermore, we make use of the ϕ dependence of $\mathcal{F}$ and employ the Jacobi-Anger expansion $e^{if\sin\phi} = \sum_{n=-\infty}^{+\infty} J_n(f) e^{in\phi}$, where $f \equiv \int_0^\zeta d\zeta' e p_\perp A(\zeta')/(kp)$. Straightforward integration of Eq. (5) leads us to the following exact form of the Volkov-Bessel state:

$$\Psi_\ell(\boldsymbol{r}, t) = \left[1 + \frac{e}{2(kp_0)}(\gamma k)(\gamma A)\right] \sum_{n=-\infty}^{+\infty} i^n J_n(f_0) \psi_{\ell+n}(\boldsymbol{r}, t), \tag{6}$$

where $f_0 \equiv f(p_0)$, and $\xi \equiv p_{\perp 0} r$ is the dimensionless transverse coordinate that defines the *width* of the EVB. Here the states

$$\psi_{\ell+n}(\boldsymbol{r}, t) = \frac{e^{i\Phi}}{\sqrt{2}} \left[\begin{pmatrix} \sqrt{1 + \frac{m}{\mathcal{E}_0}} w^s \\ \sqrt{1 - \frac{m}{\mathcal{E}_0}} \sigma_z w^s \cos\theta_0 \end{pmatrix} e^{i(\ell+n)\varphi} J_{\ell+n}(\xi) + \begin{pmatrix} 0 \\ 0 \\ \mathcal{A} \end{pmatrix} e^{i(\ell+n+1)\varphi} J_{\ell+n+1}(\xi) - \begin{pmatrix} 0 \\ 0 \\ \mathcal{B} \end{pmatrix} e^{i(\ell+n-1)\varphi} J_{\ell+n-1}(\xi) \right], \tag{7}$$

with a phase $\Phi(z, t) \equiv p_{\parallel 0} z - \mathcal{E}_0 t + \mathcal{G}(p_0)$ and spinors $\mathcal{A} \equiv (0, i\sqrt{\Delta}\alpha)^T$ and $\mathcal{B} \equiv (i\sqrt{\Delta}\beta, 0)^T$, look like the Bessel-type solution of the free Dirac equation, but with some modified OAM $\ell + n$, and where ℓ is the OAM of the (initially) field-free EVB [4]. This modified OAM arises naturally due to the *coupling* between the phase factors $e^{in\phi}$ and $e^{i\ell\phi}$. Such a coupling enables one to interpret n as an *additional* OAM due to the laser. Moreover, the state [Eq. (6)] represents a superposition of infinitely many modes $J_{\ell+n}$ and $J_{\ell+n\pm 1}$ (for a given ℓ), similar to the expression of plane waves as an infinite sum of spherical harmonics.

The presence of both the nonzero SAM and OAM of the electron gives rise to the so-called intrinsic SOI for the EVB [4]. Equation (7) shows that the coupling between the spin and angular momentum degrees of freedom is described via the modes $J_{\ell+n\pm 1}$ which appear with the coefficients $(0, 0, \mathcal{A})^T$ and $(0, 0, \mathcal{B})^T$. These coefficients, in turn, are proportional to $\sqrt{\Delta}$, where $\Delta = (1 - m/\mathcal{E}_0)\sin^2\theta_0 < 1$ is the intrinsic SOI parameter and is nonzero both in *nonparaxial* ($\theta_0 \neq 0$) and relativistic regimes. Whereas, in paraxial ($\theta_0 \to 0$) and/or in nonrelativistic ($p_0 \to 0$) limits this parameter vanishes and, therefore, the "scalar" mode $J_{\ell+n}$ remains as the only contributing term in the Volkov-Bessel states [Eqs. (6) and (7)].

It is very important to note that when we switch off the laser field, i.e., $A = 0$ and $n = 0$, we recover the results known for the field-free EVB [4,18]. On the other hand, we obtain the Dirac-Volkov solution (2) from Eqs. (6) and (7) if we consider the plane-wave limit $\theta_0 = 0$ and $\ell = 0$ for the electron, as one would expect.

Probability density of EVBs.—We can analyze the probability density of the EVB by using the Volkov-Bessel states [Eqs. (6) and (7)] to better understand how a linearly polarized laser field affects an EVB with a given energy in both nonparaxial ($\Delta < 1$) and paraxial ($\Delta \to 0$) regimes. For this, we have to use the 0th component of the four-current $j^\mu = \Psi_\ell^\dagger \gamma^0 \gamma^\mu \Psi_\ell$ [15] and evaluate

$$\rho_{\ell s} = \sum_{n,n'=-\infty}^{+\infty} J_n(f_0) J_{n'}(f_0) \Big\{ \cos\left[(n'-n)\left(\frac{\pi}{2}+\varphi\right)\right] \times \left[\left(1-\frac{\delta^2}{2}\right)\varrho_{\ell snn'} - \frac{p_{\parallel 0}\delta^2}{2\mathcal{E}_0} J_{\ell+n}J_{\ell+n'}\right] + \delta\frac{p_{\perp 0}}{\mathcal{E}_0} \times \cos\left[2s(n'-n)(\pi/2+\varphi)+\varphi\right] J_{\ell+n}J_{\ell+n'+2s}\Big\}. \quad (8)$$

Here $\delta \equiv \omega e A/(k p_0)$ is a dimensionless parameter which shows how strong or weak the laser is. Moreover,

$$\varrho_{\ell snn'} \equiv \left(1-\frac{\Delta}{2}\right) J_{\ell+n}J_{\ell+n'} + \frac{\Delta}{2} J_{\ell+n+2s}J_{\ell+n'+2s} \quad (9)$$

looks like the probability density of the field-free EVB, again with modified OAMs $\ell+n$ and $\ell+n'$. Here and in the curly brackets of Eq. (8), we omitted the argument ξ of Bessel functions, for the sake of clarity.

In our further discussion, we are interested in describing the profile of the field-affected EVB for a relatively *weak* laser with $|\delta| \ll 1$. We can therefore simplify the probability density to

$$\rho_{\ell s} \approx \sum_{n,n'=-\infty}^{+\infty} J_n(f_0) J_{n'}(f_0) \cos\left[(n'-n)\left(\frac{\pi}{2}+\varphi\right)\right] \varrho_{\ell snn'}, \quad (10)$$

that possesses a *mirror-reflection* symmetry with respect to the y axis, i.e., $\rho_{\ell s}(x) = \rho_{\ell s}(-x)$. This symmetry can be easily proved if we make the replacement $\varphi \to \pi - \varphi$ in Eq. (10), quite similar to the profile of laser-driven twisted atoms [19]. The form, Eq. (10), can be constructed also from the Volkov-Bessel states, Eqs. (6) and (7), if we approximate them via

$$\Psi_\ell(\boldsymbol{r}, t) \approx \sum_{n=-\infty}^{+\infty} \tilde{\Psi}_{\ell+n}, \tilde{\Psi}_{\ell+n} \equiv i^n J_n(f_0)\psi_{\ell+n}. \quad (11)$$

The latter expression is important for finding an "integral of motion" of laser-driven EVBs. Indeed, $\tilde{\Psi}_{\ell+n}$ are the eigenstates of the z component of the "total" angular momentum (TAM) operator $\hat{\mathcal{T}}_z \equiv \hat{\mathcal{L}}_z + \hat{\Sigma}_z$, where $\hat{\mathcal{L}}_z = -i\partial/\partial\varphi$ is the OAM operator and $\Sigma_z = 1/2\mathrm{diag}(\sigma_z, \sigma_z)$ represents the SAM operator of the electron. The corresponding eigenvalues of the TAM operator will then be $\ell + n + s$, i.e., $\hat{\mathcal{T}}_z\tilde{\Psi}_{\ell+n} = (\ell+n+s)\tilde{\Psi}_{\ell+n}$. When we switch off the laser field we get $(\hat{\mathcal{L}}_z + \hat{\Sigma}_z)\psi_\ell = (\ell+s)\psi_\ell$ [4].

To investigate the *spatiotemporal* characteristics of the EVB profile we shall here specify the shape of the four-potential A^μ. To this end, we examine a few-cycle Gaussian pulse $A = A_0 e^{-\zeta^2/a^2}\cos\zeta$ [cf. Fig. 1], where A_0 is the constant amplitude of the potential and a is the (dimensionless) *waist* size of the laser beam. For this specific waveform, f_0 can be exactly integrated and expressed by means of so-called Gauss error functions. Furthermore, to fulfill the condition $|\delta| \ll 1$, we consider a laser pulse with the electric field amplitude $E = 10^8$ V/cm, central angular frequency $\omega = 10^{16}$ Hz, and the waist size $a = 9$, corresponding to the pulse duration $\tau \approx 5.5$ fs, number of cycles $N \approx 5$ and the intensity $I \approx 1.3 \times 10^{13}$ W/cm^2 (cf. e.g., Ref. [20]). We also consider an EVB in the nonparaxial regime with the OAM $\ell = 3$, the opening angle $\theta_0 = \pi/4$, and the kinetic energy 817.4 keV corresponding to the intrinsic SOI parameter $\Delta = 0.3$ [4]. For these values, $|\delta| \lesssim 10^{-4}$ and, therefore, we can replace in very good approximation the expression Eq. (8) by the simpler form, Eq. (10). Moreover, the terms with the laser OAM greater than $n = n' = 7$ no longer contribute in Eqs. (8)–(10).

After we have chosen the parameters of the "EVB + laser" system we return to the "head-on" scenario, in which the free EVB propagates along the positive direction of z and collides with the laser pulse, localized both in z and in time t [cf. Fig. 1]. For this collision, we choose the initial condition such that the laser pulse is switched on at $t = 0$ in the transverse xy plane at $z_0 = -1100$ nm. This means that at $t \leq 0$, the EVB is described by means of the field-free state [4] [cf. Fig. 2(a)]. After the pulse passes the plane z_0, the EVB still remains field affected within the next ~1.4 femtoseconds. This period, in principle, is enough in order to reveal the influence of the field on the dynamics of the EVB profile. Figure 2 displays both the spin- and the azimuthal-dependent probability density of the EVB and its snapshot as a function of the dimensionless transverse coordinate ξ for selected time intervals. The dependence on the spin can be clearly seen in all figures due to the nonparaxiality of the relativistic EVB propagation, i.e., as a result of the intrinsic SOI in the EVB both in the presence and absence of the laser. The dependence of the probability density on the

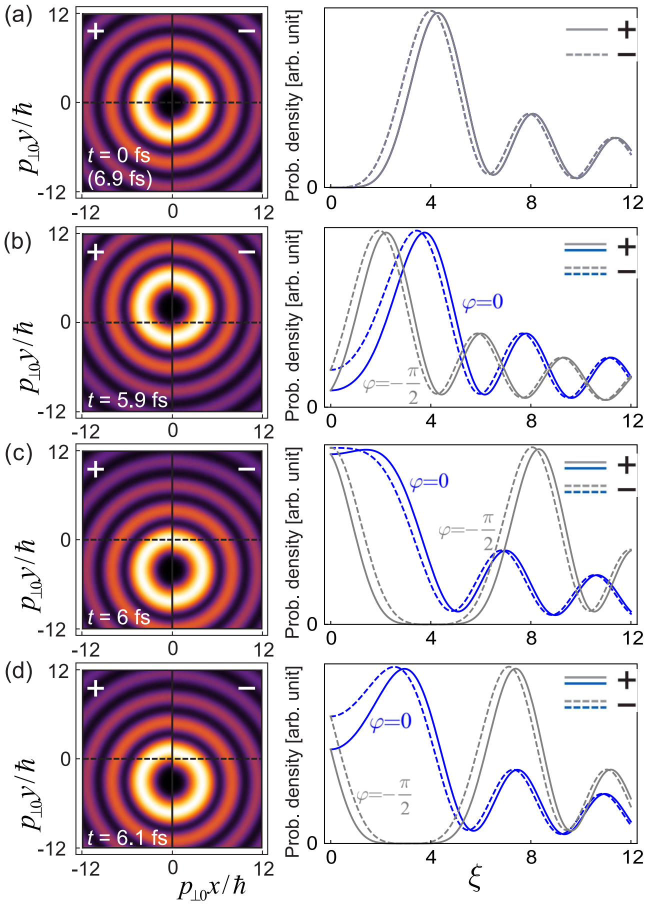

FIG. 2 (color online). Spin-, time- and azimuthal-dependent distributions of the probability density of a nonparaxial EVB (in arbitrary units of the same scale). The $s = \pm 1/2$ spin states are indicated by "+" (solid curves) and "–" (dashed curves), respectively. The snapshots of the EVB profiles are shown by the variation of colors from black to white within the "sunset" scale where black and white correspond to the minimum and maximum values of the probability density, respectively.

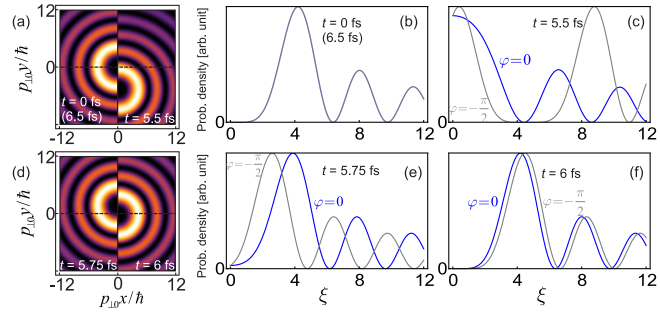

FIG. 3 (color online). Time- and azimuthal-dependent distribution of the probability density of a paraxial EVB (in arbitrary units of the same scale). The variation of colors in snapshots is the same as for Fig. 2.

azimuthal angle manifests itself in the profile of the EVB due to the electron-laser coupling [cf. Figs. 2(b)–(d) and Eq. (10)]. This φ dependence is incorporated via the *shift* of the center of the EVB with respect to the center of the (initially) field-free EVB both along the positive [Fig. 2(b)] and negative [Figs. 2(c) and 2(d)] directions of the y axis. For $t = 6$ fs, the numerical estimate of this shift gives ~0.009 nm which is the 19.9% of the beam width $\hbar\xi_0/p_{\perp 0}$, where $\xi_0 = 20$. Moreover, such a shift causes a nonzero probability for finding an electron at the center of the initially field-free beam [cf. Figs. 2(c) and 2(d)]. Finally, at $t = 6.9$ fs the EVB evolves back to the field-free EVB and, therefore, obtains the same distribution of the probability density as for $t = 0$ fs [Fig. 2(a)].

Until now, we have discussed only how the laser pulse affects the dynamics of the relativistic EVB in the non-paraxial regime. Since the first EVBs [7,21] have been constructed for electrons with energies ~200–300 keV and opening angles $\theta_0 \leq 20$ mrad, which are within the paraxial regime, we find desirable also to discuss the influence of the laser field onto the EVB dynamics for these—nowadays available—experimental parameters. We again examine the "head-on" scenario for electron and laser beams. If we consider an EVB with the OAM $\ell = 3$, opening angle $\theta_0 = 20$ mrad and the kinetic energy 300 keV, corresponding to the SOI parameter $\Delta = 0.0015$, and the few-cycle laser pulse with the same parameters as taken before, the probability density of the EVB is no longer spin dependent (Fig. 3). However, the presence of the field gives rise to a *shift* of the center of the EVB with respect to the center of the initially free paraxial beam [cf. Figs. 3(a) and 3(d)]. For $t = 5.5$ fs, this shift is ~0.02 nm which is the 20% of the *full width at half maximum diameter* of the EVB [22], thus making it accessible for measurement.

The relativistic EVB as a whole is spatially shifted along the (linear) polarization direction of the laser field, while the overall transverse structure of the (shifted) beam remains the same. Since the field oscillates in our case on a subfemtosecond time scale, the spatial shift of the beam center performs oscillations with a *similar* frequency. Additional computations show that these oscillations occur for all values of the (longitudinal) OAM ℓ and vanish only in the plane-wave limit $\ell = 0$ and $\theta_0 = 0$. Furthermore, the interaction with the laser pulse may lead to a pronounced probability to detect electrons at the (initially dark) center of the incident EVB [as seen at $\xi = 0$ in Figs. 2(c) and 2(d) and Fig. 3(c)]. Altogether, such a behavior of the beam can be interpreted classically: the EVB experiences the "standard" Lorentz force $\boldsymbol{F} = e(\boldsymbol{E} + \boldsymbol{v} \times \boldsymbol{B})$ caused by a laser field, where $\boldsymbol{v}$ is the electron velocity, $\boldsymbol{E} = -\partial \boldsymbol{A}/\partial t$ and $\boldsymbol{B} = \nabla \times \boldsymbol{A}$ are the corresponding electric and magnetic fields. As a consequence of this Lorentz-like behavior, one can control and manipulate EVBs with all the experimental techniques which have been developed over the years for other kinds of (localized) electron beams.

In conclusion, we have examined a head-on collision of two feasible beams, namely the relativistic EVB and the few-cycle laser pulse. In our formalism, we have generalized the free EVB states [4] to the laser-driven Volkov-Bessel states [Eq. (6)]. We have shown the shift of the center of the laser-driven EVB with respect to the center of the initially field-free EVB both in nonparaxial and paraxial cases. This shift is unavoidably accompanied with an azimuthal dependence of the electronic probability density distribution and can be an important observable that manifests itself in the interaction of the twisted electrons with laser pulses. We believe that recent advances in electron microscopy [8,23] will enable one to observe the above introduced effect by employing, for instance, the so-called pump-probe experiments.

A. G. H. appreciates fruitful discussions with J. Evers, R. G. Petrosyan, and T. Pfeifer and acknowledges the support from the GSI Helmholtzzentrum and the University of Heidelberg. O. M. and A. S. acknowledge support from the Helmholtz Gemeinschaft and GSI (Nachwuchsgruppe VH-NG-421).

*armen@physi.uni-heidelberg.de

[1] G. Uhlenbeck and S. Goudsmit, Naturwissenschaften **13**, 953 (1925); Nature (London) **117**, 264 (1926).
[2] V. G. Bagrov and D. M. Gitman, *Exact Solutions of Relativistic Wave Equations* (Kluwer Academic Publ., Dordrecht, Boston, London, 1990); A. Di Piazza, C. Müller, K. Z. Hatsagortsyan, and C. H. Keitel, Rev. Mod. Phys. **84**, 1177 (2012).
[3] F. H. L. Koppens, C. Buizert, K. J. Tielrooij, I. T. Vink, K. C. Nowack, T. Meunier, L. P. Kouwenhoven, and L. M. K. Vandersypen, Nature (London) **442**, 766 (2006); R. Hanson and D. D. Awschalom, *ibid.* **453**, 1043 (2008).
[4] K. Y. Bliokh, M. R. Dennis, and F. Nori, Phys. Rev. Lett. **107**, 174802 (2011).
[5] K. Y. Bliokh, Y. P. Bliokh, S. Savel'ev, and F. Nori, Phys. Rev. Lett. **99**, 190404 (2007).
[6] P. Schattschneider and J. Verbeeck, Ultramicroscopy **111**, 1461 (2011).
[7] M. Uchida and A. Tonomura, Nature (London) **464**, 737 (2010); J. Verbeeck, H. Tian, and P. Schlattschneider, *ibid.* **467**, 301 (2010); B. J. McMorran *et al.*, Science **331**, 192 (2011).
[8] J. Verbeeck, P. Schattschneider, S. Lazar, M. Stöger-Pollach, S. Löffler, A. Steiger-Thirsfeld, and G. Van Tendeloo, Appl. Phys. Lett. **99**, 203109 (2011); P. Schattschneider, B. Schaffer, I. Ennen, and J. Verbeeck, Phys. Rev. B **85**, 134422 (2012); G. Guzzinati, P. Schattschneider, K. Y. Bliokh, F. Nori, and J. Verbeeck, Phys. Rev. Lett. **110**, 093601 (2013).
[9] I. P. Ivanov, Phys. Rev. A **85**, 033813 (2012); Phys. Rev. D **85**, 076001 (2012).
[10] K. Y. Bliokh, M. A. Alonso, E. A. Ostrovskaya, and A. Aiello, Phys. Rev. A **82**, 063825 (2010).
[11] K. Y. Bliokh, A. Aiello, and M. Alonso, in *The Angular Momentum of Light*, edited by D. L. Andrews and M. Babiker (Cambridge University Press, Cambridge, England, 2013).
[12] L. Allen, M. W. Beijersbergen, R. J. C. Spreeuw, and J. P. Woerdman, Phys. Rev. A **45**, 8185 (1992).
[13] *Optical Angular Momentum*, edited by L. Allen, S. M. Barnett, and M. J. Padgett (Taylor & Francis, London, 2003); D. McGloin and K. Dholakia, Contemp. Phys. **46**, 15 (2005); *Twisted Photons: Applications of Light with Orbital Angular Momentum*, edited by J. P. Torres and L. Torner (Wiley-VCH Verlag GmbH & Co. KGaA, Weinheim, Germany, 2011).
[14] G. Molina-Terriza, J. P. Torres, and L. Torner, Nat. Phys. **3**, 305 (2007); X. Cai, J. Wang, M. J. Strain, B. Johnson-Morris, J. Zhu, M. Sorel, J. L. O'Brien, M. G. Thompson, and S. Yu, Science **338**, 363 (2012); O. Matula, A. G. Hayrapetyan, V. Serbo, A. Surzhykov, and S. Fritzsche, J. Phys. B **46**, 205002 (2013).
[15] V. B. Berestetskii, E. M. Lifshitz, and L. P. Pitaevskii, *Quantum Electrodynamics* (Pergamon, Oxford, 1982).
[16] L. D. Landau and E. M. Lifshitz, *The Classical Theory of Fields* (Pergamon, Oxford, 1975).
[17] D. V. Karlovets, Phys. Rev. A **86**, 062102 (2012).
[18] In our discussion, the normalization of the Bessel beams is not of a crucial importance. However, one can regularize the Dirac δ function, that arises after the integration of squared Bessel functions over the whole space, by rigorously redefining it as a limit of a regular function, e.g., Gaussian [4].
[19] A. G. Hayrapetyan and S. Fritzsche, Phys. Scr. **T156**, 014067 (2013); A. G. Hayrapetyan, O. Matula, A. Surzhykov, and S. Fritzsche, Eur. Phys. J. D **67**, 167 (2013).
[20] *Femtosecond Laser Pulses: Principles and Experiments*, edited by C. Rullière (Springer, New York, 2005).
[21] K. Saitoh, Y. Hasegawa, K. Hirakawa, N. Tanaka, and M. Uchida, Phys. Rev. Lett. **111**, 074801(2013).
[22] J. Verbeeck (private communication).
[23] L. Clark, A. Béché, G. Guzzinati, A. Lubk, M. Mazilu, R. Van Boxem, and J. Verbeeck, Phys. Rev. Lett. **111**, 064801 (2013); A. Winkelmann and M. Vos, *ibid.* **106**, 085503 (2011); O. L. Krivanek *et al.*, Nature (London) **464**, 571 (2010).